NASA TECHNICAL NOTE

NASA TN D-5061

NASA TN D-5061

AN ANALYTICAL PROCEDURE FOR OPTIMIZING TELEVISION SYSTEMS FOR PLANETARY DESCENT MISSIONS

by Friedrich O. Huck

Langley Research Center
Langley Station, Hampton, Va.

NATIONAL AERONAUTICS AND SPACE ADMINISTRATION • WASHINGTON, D. C. • FEBRUARY 1969

AN ANALYTICAL PROCEDURE FOR OPTIMIZING TELEVISION SYSTEMS FOR PLANETARY DESCENT MISSIONS

By Friedrich O. Huck

Langley Research Center

Langley Station, Hampton, Va.

NATIONAL AERONAUTICS AND SPACE ADMINISTRATION

For sale by the Clearinghouse for Federal Scientific and Technical Information
Springfield, Virginia 22151 – CFSTI price $3.00

AN ANALYTICAL PROCEDURE FOR OPTIMIZING TELEVISION SYSTEMS FOR PLANETARY DESCENT MISSIONS

By Friedrich O. Huck
Langley Research Center

SUMMARY

An analytical procedure is developed for optimizing spacecraft television systems to secure proper overlap between successive pictures and maximum surface resolution during planetary descent. The television characteristics of concern are optical field of view and number of scan lines. Results show how the optimum combination of these characteristics depends on target brightness, camera sensitivity, transmission rate, and spacecraft trajectory values.

INTRODUCTION

It is generally desirable that the pictures which are to be obtained from a spacecraft during lunar or planetary descent overlap in surface coverage to provide continuous surface information and to locate the landing point. Lunar luminance, approach velocity, and the resulting image smear were important factors in the design of a television system for obtaining high-resolution pictures of the lunar surface for the impacting mission of the Ranger spacecraft (ref. 1). The available transmission bandwidth was not a limiting factor. However, for the more distant planetary descent missions such as a landing on Mars (ref. 2), the available transmission bandwidth becomes a dominant limitation to obtaining both high-resolution and overlapping pictures.

In this paper an analytical procedure is developed for optimizing television camera characteristics to secure proper overlap between successive pictures and maximum surface resolution under real-time data transmission constraints. The television characteristics of concern are optical field of view and number of scan lines. Proper overlap between successive pictures is specified by the minimum number of balanced scan lines required in the overlapping surface area of two image frames; a larger overlap would result in the transmission of wasteful data, and a smaller overlap could result in the failure of correlating successive pictures and hence in locating the landing site.

SYMBOLS

A	area, meters^2
A_o	area common to two successive image frames, meters^2
C	video system capacity, bits/second
E	exposure, meter-candle-seconds
f_n	focal ratio or "f-number"
F	average value of the two bases of a trapezoid, meters
F_1	short base of trapezoid, meters (see fig. 6)
F_2	long base of trapezoid, meters (see fig. 6)
g	phase angle, angle between incident light and camera optical axis, degrees (see fig. 6)
G	altitude of trapezoid, meters (see fig. 6)
H	altitude, meters
I	information storage capacity of an image frame, bits
I_o	information storage capacity inherent in the common area of two overlapping image frames, bits
j	variable that defines sequence of image frames
k	constant relating photoconductor erase-and-prepare time to readout time
K	solar illumination constant, meter-candles
m	number of binary digits used for encoding shades of grey, bits
n	surface normal

N	number of balanced scan lines per frame, $\left(N_h \times N_v\right)^{1/2}$
N_h	number of elements per scan line
N_ℓ	lowest desirable number of balanced scan lines for television system
N_v	number of scan lines per frame
N_o	number of balanced scan lines contained in the overlapping area of two image frames
R	resolution, meters/optical line pair
R_s	resolution degraded by smear, meters
S	smear, meters
t	time, seconds
t_e	erase-and-prepare time, seconds
t_E	exposure time, seconds
t_p	time interval between the exposure of two successive images, seconds
t_r	transmission or readout time for one image frame, seconds
T	transmission rate, bits/second
v	velocity, meters/second
v_h	horizontal component of spacecraft velocity vector, meters/second
v_v	vertical component of spacecraft velocity vector, meters/second
x,y,z	linear distances, meters
γ	flight-path angle, degrees (see fig. 8)

ϵ	angle between optical axis and surface normal, degrees (see fig. 6)
ζ	optical full field of view, degrees
ι	angle between incident illumination and surface normal, degrees (see fig. 6)
ξ	angle between spacecraft velocity vector and optical axis, degrees (see fig. 8)
ρ	normal albedo of a surface
τ	white light lens transmission
$\phi(\epsilon,\iota,g)$	illumination scattering function
$< >$	average value

ASSUMPTIONS

The analysis presented in this paper is subject to the following assumptions:

1. Spacecraft movement is restricted to point-mass trajectory motion as was that for the impacting mission of the Ranger spacecraft (ref. 1). A more general analysis which would include all possible spacecraft dynamics is very complex; however, the optimization of camera characteristics can be demonstrated for this simpler case.

2. For the purpose of this analysis, the spacecraft trajectory parameters are specified by altitude, velocity, and flight-path angle. The variation of these parameters during planetary descent causes a variation in the transmission rate required to secure proper image overlap (ref. 2). The analytical procedure developed here is best applied to that part of the descent trajectory which requires the highest transmission rate.

3. Image information is transmitted directly as it is scanned off the photoconductor surface of an electro-optical imaging device, such as the slow-scan vidicons used in the Ranger television system (ref. 1). Transmission of image information before impact is, of course, required for a mission in which the spacecraft is not designed to survive. It is also desirable for a landing mission in which the spacecraft is designed to survive because the possibility of landing failure cannot be disregarded. Moreover, real-time data transmission alleviates the necessity for any storage device, such as a tape recorder.

4. Since the photoconductor erase-and-prepare time and readout time are fixed by system design and are usually not varied during a mission, they are related by an appropriate positive constant.

ANALYSIS

The analysis is divided into two parts. In the first part an expression is derived for the transmission rate required to secure proper overlap between successive pictures. An example is given to illustrate the selection of the combinations of camera field of view and number of television scan lines which provide proper picture overlap for a given transmission rate. In the second part a procedure is presented for selecting that combination of field of view and number of scan lines which also secures maximum surface resolution. This procedure is also illustrated by an example.

Image Overlap and Transmission Rate Requirement

The maximum possible information content of a picture depends on the number of resolvable elements in the image frame and on the number of distinguishable intensity levels in each element. The number of elements N^2 contained in an image frame is given by the product of the number of scan lines per frame N_v and the number of elements per line N_h. The parameter N is referred to herein as the number of balanced scan lines per frame. If each element is encoded to 2^m shades of grey, then the information storage capacity of an image frame is at most, in bits of information,

$$I = mN_hN_v = mN^2 \tag{1}$$

Similarly, the maximum information which can be contained in that area of one image frame which is common to another may be given by $I_o = mN_o^2$ where N_o^2 is the number of elements in the common area of one of the frames. Because successive pictures are generally obtained from different altitudes, each has a different number of elements in the area which is common to the next picture in succession. (See fig. 1.) Obviously, the lower value of N_o is critical and is, therefore, used to specify proper overlap.

A design requirement for N_o must be based on the amount of detail and contrast expected in the scene to be imaged. Unless a priori terrain information is available, a minimum requirement cannot be established rigorously.

The capacity of a television and communication system to acquire and transmit video information in bits/sec is

$$C = \frac{I}{t_p} = \frac{mN^2}{t_p} \tag{2}$$

where t_p is the time interval between the exposure of two successive images. The required transmission rate in bits/sec is

$$T = \frac{I}{t_r} = \frac{mN^2}{t_r} \tag{3}$$

where t_r is the readout time for one image frame. This expression for transmission rate does not include the line and frame synchronization.

The parameters t_r and t_p are related simply by

$$t_p = t_r + t_e + t_E \tag{4}$$

where t_e is the photoconductor erase-and-prepare time and t_E is the exposure time. The exposure time is usually several orders of magnitude smaller than either t_r or t_e and therefore will be disregarded here. Since t_r and t_e are related by a positive constant, equation (4) can be expressed in the form

$$t_r = t_p - kt_r = \frac{t_p}{k + 1} \tag{5}$$

If, for example, erase-and-prepare time equals readout time, then $k = 1$ and $t_r = t_p/2$. When this occurs, two vidicons could be used alternately to transmit information and erase and prepare their photoconductor surface, and the required transmission rate could then be reduced to the required system capacity.

Substituting equation (5) into equation (3) yields the following expression for the transmission rate:

$$T = \frac{(k + 1)mN^2}{t_p} \tag{6}$$

The derivation of an expression for the time interval t_p required to secure a proper overlap between successive pictures N_o is presented in appendix A as a function of spacecraft trajectory parameters, camera characteristics, and viewing geometry.

To illustrate the selection of the combinations of optical field of view and number of scan lines which provide proper picture overlap for a given transmission rate, an example is considered. If it is assumed that the spacecraft velocity-over-height ratio does not change significantly between two successive pictures and that the camera viewing geometry remains nearly vertical, then upon substituting equation (A19) for t_p into equation (6), the transmission rate becomes

$$T = \frac{\left[2(k + 1)mN^2\right] \frac{v_v}{H}\left(\frac{v_v}{H} + \frac{v_h}{H \tan \frac{\zeta}{2}}\right)}{\left(3 \frac{v_v}{H} + \frac{v_h}{H \tan \frac{\zeta}{2}}\right) - \left[\left(\frac{v_v}{H} - \frac{v_h}{H \tan \frac{\zeta}{2}}\right)^2 + 8 \frac{N_o^2}{N^2} \frac{v_v}{H}\left(\frac{v_v}{H} + \frac{v_h}{H \tan \frac{\zeta}{2}}\right)\right]^{1/2}} \tag{7a}$$

providing $v_V \neq 0$; if $v_V = 0$, then by using equation (A20)

$$T = \frac{(k + 1)mN^2 v_h}{2H\left(1 - \frac{N_o^2}{N^2}\right)\tan\frac{\zeta}{2}} \tag{7b}$$

The variation of T as given by equation (7a) with optical field of view and number of balanced scan lines is plotted in figure 2. Assumed are spacecraft velocity-over-height ratios of $\frac{v_h}{H} = \frac{v_V}{H} = 0.01\ \text{sec}^{-1}$, a brightness word of $m = 6$ bits, and the constant $k = 1$. By considering, for example, a transmission rate of $15N_o^2$ bits/sec, proper overlap is provided by $\zeta = 2^o$ and $N = 1.63N_o$ lines or by $\zeta = 4^o$ and $N = 2.68N_o$ lines, and so on. Furthermore, a value slightly less than 2^o presents the lowest field of view which can secure proper overlap under the given conditions, regardless of the number of scan lines used.

It can be shown analytically, as well as seen in figure 2, that T approaches infinity as N approaches either N_o or infinity and that one minimum value exists between these two extremes. The number of balanced scan lines corresponding to this minimum value N_l is an important quantity because any lower scan-line value would reduce image resolution and increase the required transmission rate.

Since for the variation of T with changes in N a single minimum value occurs, N_l can be found directly by solving $\frac{d}{dN}T = 0$ for N. This solution is presented in appendix B where the expression for T given by equation (7a) is used with the following result:

$$N_l = N_o \frac{\left[\left(\frac{v_h^2}{\tan^2\frac{\zeta}{2}} - \frac{6v_h v_V}{\tan\frac{\zeta}{2}} - 3v_V^2\right) + \left(3v_V + \frac{v_h}{\tan\frac{\zeta}{2}}\right)\left(3v_V^2 + \frac{v_h^2}{\tan^2\frac{\zeta}{2}}\right)^{1/2}\right]^{1/2}}{v_V + \frac{v_h}{\tan\frac{\zeta}{2}}} \tag{8a}$$

When the vertical velocity component v_V is equal to zero,

$$N_l = \sqrt{2}\,N_o = 1.41N_o \tag{8b}$$

And when the horizontal velocity component v_h is equal to zero,

$$N_l = \sqrt{3\left(\sqrt{3} - 1\right)}N_o = 1.48N_o \tag{8c}$$

Equation (8a) reveals that N_ℓ is dependent on spacecraft velocity and optical field of view and independent of altitude and the constant k. When either v_h or v_v is zero, N_ℓ is related to N_o simply by a constant as given in equations (8b) and (8c).

To determine the variation of N_ℓ with changes in these parameters, equation (8a) was computer programed and evaluated for a wide range of values for v_h, v_v, and ζ. Some typical results are plotted in figure 3 to illustrate this variation. For this example all values for N_ℓ were contained within a range extending from $1.41N_o$ to $1.50N_o$.

Image Resolution and Smear

The foregoing procedure for selecting combinations of optical field of view and number of scan lines which provide proper overlap between successive pictures is now extended for determining the combination of ζ and N which also secures maximum surface resolution. The relationships used in this section for geometrical resolution, resolution degradation by smear, and proper photoconductor exposure have been derived and discussed in detail in reference 3.

Geometrical ground resolution is given by

$$R = \frac{2.8H\left(2 \tan \frac{\zeta}{2}\right)}{N \cos^2 \epsilon} \tag{9}$$

Camera motion during exposure degrades this resolution by causing smear. The smear due to the point-mass motion of a spacecraft can be divided into two components: smear due to translational motion perpendicular to the optical axis (linear smear) and smear due to translational motion parallel to the optical axis (zoom effect or edge blur). Edge blur is caused by the motion of the camera toward or away from the target and appears in the form of points moving radially to or from the center of the picture. It is zero at the center of the picture and maximum at the edges. Since linear smear is unidirectional and edge blur is multidirectional, the two smear components may either tend to compensate for each other or may add linearly.

Image smear is most critical at the edge of the image frame where overlap between successive pictures must be attained. It is, therefore, appropriate to use the sum of linear smear and maximum edge blur in determining smear, as given by

$$S = \frac{\left(v \sin \xi + v \cos \xi \tan \frac{\zeta}{2}\right) t_E}{\cos \epsilon} \tag{10}$$

Since the amount of image smear is directly proportional to exposure time t_E, it is desirable to reduce this time interval as much as the image sensor and optics permit.

Target brightness, photoconductor sensitivity, optical characteristics, and exposure time are related by the expression obtained from reference 3

$$E = \frac{K\rho\phi(\epsilon,\iota,g)\tau t_E}{4f_n^2} \tag{11}$$

The factors K, ρ, and $\phi(\epsilon,\iota,g)$ pertain to the radiometric properties of the solar illumination and the planetary surface and the remaining factors to camera characteristics.

Of the planetary properties, only the illumination scattering function $\phi(\epsilon,\iota,g)$ may be controlled by varying the angular relation between the camera optical axis, incident illumination, and surface normal.

Of the camera characteristics, the exposure E must be chosen to provide a sufficient signal-to-noise ratio from the photocathode of the electro-optical imaging device. The white light lens transmission τ ranges from 50 percent to over 80 percent with 70 percent being a good average and is generally not a critical factor in camera design. The lens f-number f_n is a measure of the lens light-gathering ability and as such is an important parameter to this analysis. The lower limit in f-number of lenses currently available for a 11.2-mm square vidicon format as a function of optical field of view is plotted in figure 4 from data given in reference 4. This variation in the lower limit of f-number occurs because aberrations scale up for the long focal length required for small angular fields and control of the aberrations is difficult for large angular fields.

Solving equation (11) for t_E, substituting the resulting expression into equation (10), and then adding equation (10) to (9) yields the following relation for resolution degraded by smear

$$R_S = \frac{2.8H\left(2\tan\frac{\zeta}{2}\right)}{N\cos^2\epsilon} + \frac{v\sin\xi + v\cos\xi\tan\frac{\zeta}{2}}{\cos\epsilon}\,\frac{4f_n^2E}{K\rho\phi(\epsilon,\iota,g)\tau} \tag{12}$$

To illustrate the selection of an optimum combination of optical field of view and number of scan lines which secures both proper picture overlap and maximum surface resolution, the example considered previously is now continued. Spacecraft altitude H is assumed to be 10 000 meters, velocities v_h and v_v are assumed to be 100 m/sec, and thus the velocity-over-height ratios v_h/H and v_v/H are 0.01 sec^{-1}. It is further assumed that proper picture overlap N_O is secured by 100 balanced scan lines, that the transmission rate T is $15N_O^2$ which equals 150 000 bits/sec, and that the slow-scan vidicon television characteristics and Martian imaging conditions summarized from reference 2 in table I are applicable. (The illumination scattering function for Mars, however, is not well known even after the analysis of Mariner IV pictures (ref. 5). This

function is believed to lie between that for a Lambertian reflector and that for the lunar surface.) A Martian environment is chosen because the planet's thin and sparsely clouded atmosphere presents a favorable condition to imaging.

Under these assumptions, equation (12) reduces to

$$R_S = \frac{56\ 000 \tan \frac{\zeta}{2}}{N} + 0.4\left(1 + \tan \frac{\zeta}{2}\right) f_n^2 \tag{13}$$

The variation of resolution with and without the effect of smear is plotted in figure 5. Maximum surface resolution without the effect of smear is provided by a television system which contains the lowest number of balanced scan lines N_l and the lowest field of view which still allows the required overlap at the given transmission rate. Maximum surface resolution degraded by smear is provided by a higher number of scan lines and a wider field of view. The width of the area covered by an image frame is also plotted to illustrate how the gain in resolution is paid for by loss in coverage.

CONCLUDING REMARKS

An analytical procedure was developed for optimizing spacecraft television systems for planetary descent missions. This procedure provides an optimum combination of optical field of view and number of scan lines which secures proper overlap between successive pictures and maximum surface resolution. This optimum combination depends on target brightness, camera sensitivity, transmission rate, and spacecraft trajectory values.

An example of this procedure indicates that proper picture overlap, defined by N_O balanced scan lines, and maximum surface resolution without considering smear are secured by a television system which contains a number of balanced scan lines between $1.41N_O$ and $1.50N_O$ and the lowest field of view which still provides the proper overlap for a given transmission rate. When resolution degradation by smear is considered, the optimum combination of television parameters tends toward a higher number of scan lines and a wider field of view.

Langley Research Center,
National Aeronautics and Space Administration,
Langley Station, Hampton, Va., November 6, 1968,
125-24-01-11-23.

APPENDIX A

DERIVATION OF THE TIME INTERVAL BETWEEN EXPOSURES FOR SECURING A REQUIRED OVERLAP BETWEEN SUCCESSIVE PICTURES

Successive pictures obtained from a moving spacecraft are required to overlap by a specified amount. An expression is derived in this appendix for the maximum allowable time interval between exposures of two successive image frames and is followed by two approximations. The first approximation is for the case where viewing geometry and spacecraft velocity change insignificantly during this time interval; the second approximation is for the case of vertical viewing geometry.

Viewing geometry and surface coverage are shown in figure 6. One side of the square photoconductor format is assumed to be parallel to the spacecraft flight path. The resulting surface coverage takes the form of a trapezoid for a nonvertical viewing geometry. To simplify the derivation, this trapezoid is approximated by a rectangle. In this approximation, the altitude of the trapezoid G becomes the length of the rectangle along the direction of the spacecraft flight path, and the average of the two bases of the trapezoid F_1 and F_2 becomes the width of the rectangle perpendicular to the flight path. This average width is given by $F = \frac{1}{2}(F_1 + F_2)$. It may be noted that the total surface coverage has not been changed by this approximation.

As indicated in figure 1, two successive images must share a certain amount of surface information in order that these images may be matched. Each image has an information storage capacity given by $I = mN^2$.

The information storage capacity of the surface area A_o common to both images due to picture j is

$$I_{o,j} = \frac{mN^2 A_o}{A_j} \tag{A1}$$

and due to picture $j + 1$ is

$$I_{o,j+1} = \frac{mN^2 A_o}{A_{j+1}} \tag{A2}$$

For a descending spacecraft, $A_j \geqq A_{j+1}$ and therefore $I_{o,j} \leqq I_{o,j+1}$. Since the lower value of information about the surface area common to two successive images is critical, the overlap requirement is specified by $I_{o,j} \equiv I_o$. By referring to figure 7, equation (A1) may be rewritten in the form

$$\frac{x_{j,j+1} F_{j+1}}{F_j G_j} = \frac{N_o^2}{N^2} \tag{A3}$$

where N_o^2 is the number of scan elements contained in the area A_o due to picture j.

APPENDIX A

The dimension $y_{j,j+1}$, as obtained from figure 7 is

$$y_{j,j+1} = \frac{1}{2}\left(G_j + G_{j+1}\right) - x_{j,j+1} \tag{A4}$$

and as obtained from figure 8 is

$$y_{j,j+1} = z_{j,j+1} - H_j \tan \epsilon_j + H_{j+1} \tan \epsilon_{j+1} \tag{A5}$$

Equating the right side of equations (A4) and (A5), and substituting for $x_{j,j+1}$ by the expression given in equation (A3) yields

$$z_{j,j+1} - H_j \tan \epsilon_j + H_{j+1} \tan \epsilon_{j+1} = \frac{1}{2}\left(G_j + G_{j+1}\right) - \frac{N_o^2}{N^2} \frac{F_j G_j}{F_{j+1}} \tag{A6}$$

By using the viewing geometry shown in figure 6 and the approximation $F = \frac{1}{2}\left(F_1 + F_2\right)$, the dimensions of picture coverage are given as

$$F_j = H_j \left[\frac{\tan \frac{\zeta}{2}}{\cos\left(\epsilon_j - \frac{\zeta}{2}\right)} + \frac{\tan \frac{\zeta}{2}}{\cos\left(\epsilon_j + \frac{\zeta}{2}\right)} \right] \tag{A7}$$

$$G_j = H_j \left[\tan\left(\epsilon_j + \frac{\zeta}{2}\right) - \tan\left(\epsilon_j - \frac{\zeta}{2}\right) \right] \tag{A8}$$

$$F_{j+1} = H_{j+1} \left[\frac{\tan \frac{\zeta}{2}}{\cos\left(\epsilon_{j+1} - \frac{\zeta}{2}\right)} + \frac{\tan \frac{\zeta}{2}}{\cos\left(\epsilon_{j+1} + \frac{\zeta}{2}\right)} \right] \tag{A9}$$

$$G_{j+1} = H_{j+1} \left[\tan\left(\epsilon_{j+1} + \frac{\zeta}{2}\right) - \tan\left(\epsilon_{j+1} - \frac{\zeta}{2}\right) \right] \tag{A10}$$

It is convenient to define the time interval between the exposure of two successive images as $t_p = \left| t_j - t_{j+1} \right|$ and the average horizontal spacecraft velocity component during that time as

$$\langle v_h \rangle \equiv \langle v_h \rangle_{j,j+1} = \frac{1}{t_p} \int_{t_j}^{t_{j+1}} v(t) \cos \gamma(t) dt \tag{A11}$$

and, similarly, the average vertical velocity component as

$$\langle v_v \rangle \equiv \langle v_v \rangle_{j,j+1} = \frac{1}{t_p} \int_{t_j}^{t_{j+1}} v(t) \sin \gamma(t) dt \tag{A12}$$

By using these definitions, the parameter $z_{j,j+1}$ can be written as

$$z_{j,j+1} = \langle v_h \rangle t_p \tag{A13}$$

and the altitudes H_j and H_{j+1} are related by

$$H_{j+1} = H_j - \langle v_v \rangle t_p \tag{A14}$$

An expression for t_p is derived by substituting equations (A13) and (A14) into equation (A6) as follows:

$$\langle v_h \rangle t_p - H_j \tan \epsilon_j + H_j \tan \epsilon_{j+1} - \langle v_v \rangle t_p \tan \epsilon_{j+1}$$

$$= \frac{1}{2}\left(\frac{G_j}{H_j}\right)H_j + \frac{1}{2}\left(\frac{G_{j+1}}{H_{j+1}}\right)\left(H_j - \langle v_v \rangle t_p\right) - \frac{N_o^2}{N^2}\frac{\left(\frac{F_j}{H_j}\right)\left(\frac{G_j}{H_j}\right)H_j^2}{\left(\frac{F_{j+1}}{H_{j+1}}\right)\left(H_j - \langle v_v \rangle t_p\right)} \tag{A15}$$

The ratios F_j/H_j, G_j/H_j, F_{j+1}/H_{j+1}, and G_{j+1}/H_{j+1} can be obtained from equations (A7) to (A10). These ratios are independent of velocity and altitude and dependent only on the viewing geometry of pictures j and $j + 1$. Solving equation (A15) for t_p yields a quadratic equation which has the solution

$$t_p = \frac{1}{2a}\left(b - \sqrt{b^2 - 4ac}\right) \tag{A16a}$$

providing that $\langle v_v \rangle \neq 0$; if $\langle v_v \rangle = 0$, then

$$t_p = \frac{c}{b} \tag{A16b}$$

where

$$a = \langle v_v \rangle \left\{ \langle v_v \rangle \left[\frac{1}{2}\left(\frac{G_{j+1}}{H_{j+1}}\right) - \tan \epsilon_{j+1} \right] + \langle v_h \rangle \right\}$$

$$b = H_j \left\{ \langle v_v \rangle \left[\frac{1}{2}\left(\frac{G_j}{H_j}\right) + \frac{G_{j+1}}{H_{j+1}} + \tan \epsilon_j - 2 \tan \epsilon_{j+1} \right] + \langle v_h \rangle \right\}$$

$$c = H_j^2 \left[\frac{1}{2}\left(\frac{G_j}{H_j}\right) + \frac{1}{2}\left(\frac{G_{j+1}}{H_{j+1}}\right) + \tan \epsilon_j - \tan \epsilon_{j+1} - \frac{N_o^2}{N^2}\frac{\left(\frac{F_j}{H_j}\right)\left(\frac{G_j}{H_j}\right)}{\left(\frac{F_{j+1}}{H_{j+1}}\right)} \right]$$

APPENDIX A

Approximation 1

For portions of the trajectory where the viewing geometry and spacecraft velocity change only insignificantly during the time interval t_p, that is, where $\epsilon_j \approx \epsilon_{j+1}$ and $\langle v \rangle_{j,j+1} \approx v_{j+1} \approx v_j$, the parameters a, b, and c of equations (A16) can be approximated by a simple expression. In this approximation

$$\frac{F_j}{H_j} = \frac{F_{j+1}}{H_{j+1}} = \frac{\tan\frac{\zeta}{2}}{\cos\left(\epsilon - \frac{\zeta}{2}\right)} + \frac{\tan\frac{\zeta}{2}}{\cos\left(\epsilon + \frac{\zeta}{2}\right)} \tag{A17}$$

and

$$\frac{G_j}{H_j} = \frac{G_{j+1}}{H_{j+1}} = \tan\left(\epsilon_j + \frac{\zeta}{2}\right) - \tan\left(\epsilon_j - \frac{\zeta}{2}\right) \tag{A18}$$

Substituting equations (A17) and (A18) into the expressions for a, b, and c of equations (A16) yields

$$a = v_{v,j}\left\{v_{v,j}\left[\tan\left(\epsilon_j + \frac{\zeta}{2}\right) - \tan\left(\epsilon_j - \frac{\zeta}{2}\right) - 2\tan\epsilon_j\right] + 2v_{h,j}\right\}$$

$$b = H_j\left\{v_{v,j}\left[3\tan\left(\epsilon_j + \frac{\zeta}{2}\right) - 3\tan\left(\epsilon_j - \frac{\zeta}{2}\right) - 2\tan\epsilon_j\right] + 2v_{h,j}\right\}$$

$$c = 2H_j^2\left(1 - \frac{N_o^2}{N^2}\right)\left[\tan\left(\epsilon_j + \frac{\zeta}{2}\right) - \tan\left(\epsilon_j - \frac{\zeta}{2}\right)\right]$$

Approximation 2

If near-vertical viewing geometry is considered, that is, $\epsilon_j \approx 0$, an additional approximation can be made by letting

$$a = v_{v,j}\left(v_{v,j} + \frac{v_{h,j}}{\tan\frac{\zeta}{2}}\right)$$

$$b = H_j\left(3v_{v,j} + \frac{v_{h,j}}{\tan\frac{\zeta}{2}}\right)$$

$$c = 2H_j^2\left(1 - \frac{N_o^2}{N^2}\right)$$

If these quantities for a, b, and c are substituted into equations (A16), the time interval t_p can be written as

$$t_p = \frac{\left(3\frac{v_{v,j}}{H_j} + \frac{v_{h,j}}{H_j \tan\frac{\zeta}{2}}\right) - \left[\left(3\frac{v_{v,j}}{H_j} + \frac{v_{h,j}}{H_j \tan\frac{\zeta}{2}}\right)^2 - 8\left(1 - \frac{N_o^2}{N^2}\right)\frac{v_{v,j}}{H_j}\left(\frac{v_{v,j}}{H_j} + \frac{v_{h,j}}{H_j \tan\frac{\zeta}{2}}\right)\right]^{1/2}}{2\frac{v_{v,j}}{H_j}\left(\frac{v_{v,j}}{H_j} + \frac{v_{h,j}}{H_j \tan\frac{\zeta}{2}}\right)}$$

or

$$t_p = \frac{\left(3\frac{v_{v,j}}{H_j} + \frac{v_{h,j}}{H_j \tan\frac{\zeta}{2}}\right) - \left[\left(\frac{v_{v,j}}{H_j} - \frac{v_{h,j}}{H_j \tan\frac{\zeta}{2}}\right)^2 + 8\frac{N_o^2}{N^2}\frac{v_{v,j}}{H_j}\left(\frac{v_{v,j}}{H_j} + \frac{v_{h,j}}{H_j \tan\frac{\zeta}{2}}\right)\right]^{1/2}}{2\frac{v_{v,j}}{H_j}\left(\frac{v_{v,j}}{H_j} + \frac{v_{h,j}}{H_j \tan\frac{\zeta}{2}}\right)} \qquad \text{(A19)}$$

providing $v_{v,j} \neq 0$; if $v_{v,j} = 0$, then

$$t_p = \frac{2\left(1 - \frac{N_o^2}{N^2}\right)}{\frac{v_{h,j}}{H_j \tan\frac{\zeta}{2}}} \qquad \text{(A20)}$$

APPENDIX B

DERIVATION OF AN EXPRESSION FOR THE LOWEST DESIRABLE NUMBER OF SCAN LINES

As illustrated in figure 2, the transmission rate required to obtain an overlap of N_o^2 scan elements between successive images varies with the number of balanced scan lines N used. Transmission rate approaches infinity as N approaches either N_o or infinity and exhibits a single minimum value between these extremes. The number of scan lines corresponding to this minimum value of transmission rate was defined as the lowest desirable number of scan lines and designated by N_l.

An expression for N_l can be derived by letting $\frac{d}{dN} T = 0$ and solving for N. The expression for the transmission rate T given by equation (7a) is used in this derivation. This equation is more conveniently expressed for this purpose in the form

$$T = \frac{eN^2}{f - \left(g + hN^{-2}\right)^{1/2}} \tag{B1}$$

where

$$e = \frac{2(k+1)mv_v\left(v_v + \frac{v_h}{\tan\frac{\zeta}{2}}\right)}{H}$$

$$f = 3v_v + \frac{v_h}{\tan\frac{\zeta}{2}}$$

$$g = \left(v_v - \frac{v_h}{\tan\frac{\zeta}{2}}\right)^2$$

$$h = 8N_o^2 v_v\left(v_v + \frac{v_h}{\tan\frac{\zeta}{2}}\right)$$

If $u = eN^2$ and $w = f - \left(g + hN^{-2}\right)^{1/2}$, then

$$\frac{dT}{dN} = \frac{1}{w^2}\left(w\frac{du}{dN} - u\frac{dw}{dN}\right) = 0$$

or

$$w \frac{du}{dN} - u \frac{dw}{dN} = 0 \tag{B2}$$

Performing the operation indicated by equation (B2) and solving for N yields

$$N_\ell^2 = \frac{-h\left[\left(f^2 - 3g\right) \pm f\left(f^2 + 3g\right)^{1/2}\right]}{2g\left(f^2 - g\right)} \tag{B3}$$

Substituting values for f, g, and h yields the final result

$$N_\ell^2 = N_o^2 \frac{\left(\frac{v_h^2}{\tan^2 \frac{\zeta}{2}} - \frac{6v_h v_v}{\tan \frac{\zeta}{2}} - 3v_v^2\right) + \left(3v_v + \frac{v_h}{\tan \frac{\zeta}{2}}\right)\left(3v_v^2 + \frac{v_h^2}{\tan^2 \frac{\zeta}{2}}\right)^{1/2}}{\left(v_v - \frac{v_h}{\tan \frac{\zeta}{2}}\right)^2} \tag{B4}$$

In going from equation (B3) to (B4), the correct sign in front of the square root can be selected either by comparing the two possible results with the example illustrated in figure 2 or by considering the case where v_h or v_v equals zero. If $v_v = 0$ and $v_h \neq 0$, equation (B4) reduces to

$$N_\ell^2 = \left(1 \pm \sqrt{1}\right) N_o^2$$

And if $v_h = 0$ and $v_v \neq 0$, equation (B4) reduces to

$$N_\ell^2 = 3\left(-1 \pm \sqrt{3}\right) N_o^2$$

The negative sign in front of the square root would reduce N_ℓ^2 either to zero or to a negative quantity which is physically meaningless. The positive sign is therefore correct.

REFERENCES

1. Kindt, Donald H.; and Staniszewski, Joseph R.: The Design of the Ranger Television System to Obtain High-Resolution Photographs of the Lunar Surface. Tech. Rep. No. 32-717 (Contract No. NAS 7-100), Jet Propulsion Lab., California Inst. Technol., Mar. 1, 1965.

2. Huck, Friedrich O.; Kopia, Leonard P.; and Spiers, Robert B., Jr.: Requirements of a Martian Television Experiment for Three Point-Mass Descent Trajectories. NASA TN D-5062, 1969.

3. Herriman, A. G.; Washburn, H. W.; and Willingham, D. E.: Ranger Preflight Science Analysis and the Lunar Photometric Model. Tech. Rep. No. 32-384 (Rev.) (Contract No. NAS 7-100), Jet Propulsion Lab., California Inst. Technol., Mar. 11, 1963.

4. Tuttle, Clifton, M., ed.: The Optical Industry and Systems Directory. The Optical Pub. Co., Inc., c.1966, pp. 331-354.

5. Leighton, Robert B.; Murray, Bruce C.; et al.: Mariner Mars 1964 Project Report: Television Experiment. Part I. Investigators' Report. Tech. Rep. No. 32-884 (Contract No. NAS 7-100), Jet Propulsion Lab., California Inst. Technol., Dec. 15, 1967.

TABLE I.- NOMINAL VALUES USED TO CALCULATE EXPOSURE TIME

[Ref. 2]

E, vidicon exposure, m-c-sec	1.0
f_n, f-number	Given in figure 4
K, solar illumination constant at Mars during favorable opposition, m-c	6.7×10^4
ρ, albedo integrated over visual spectrum of Mars	0.154
τ, white light lens transmission	0.7
$\phi(\epsilon, \iota, g)$, illumination scattering function for lunar surface at $\epsilon = 0^o$, $\iota = g = 70^o$	[a]0.14

[a]The illumination scattering function for Mars is not well known even after the analysis of Mariner IV pictures (ref. 5). This function is believed to lie between that for a Lambertian reflector and that for the lunar surface.

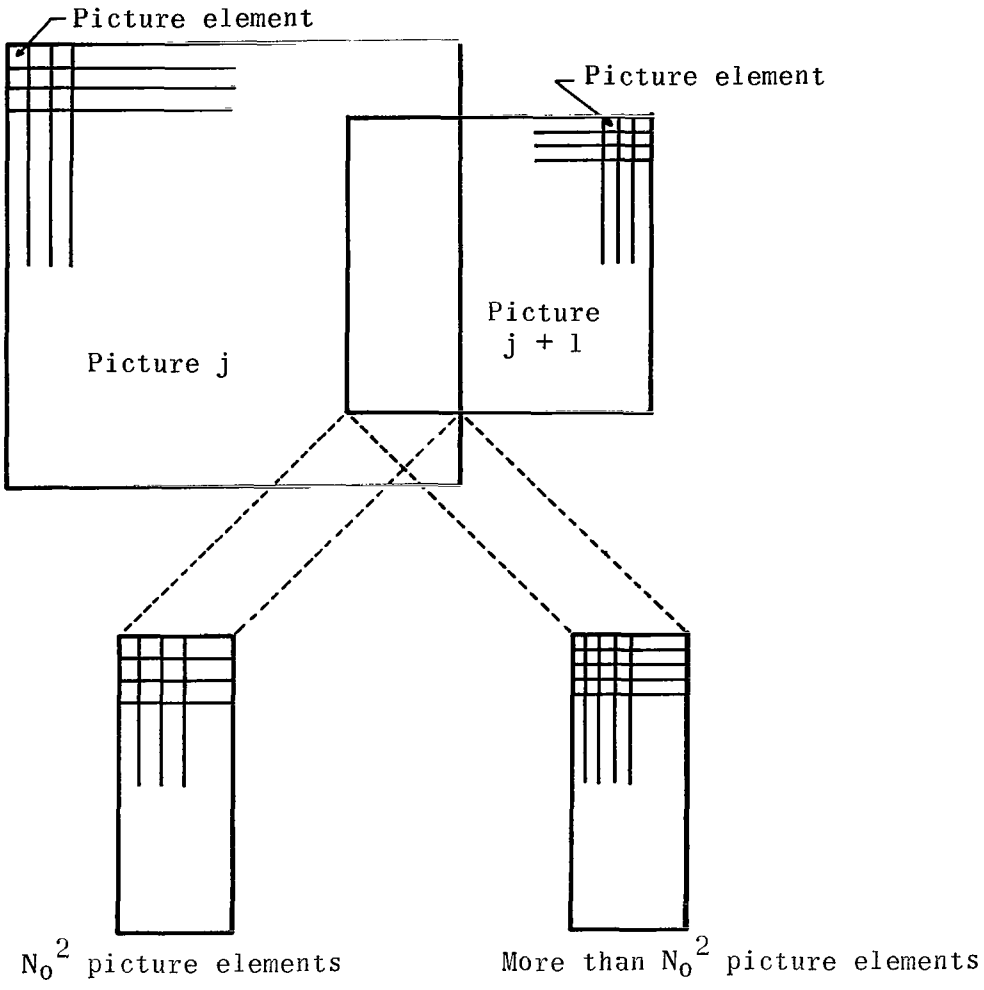

Figure 1.- Footprint of two successive pictures to illustrate proper surface overlap.

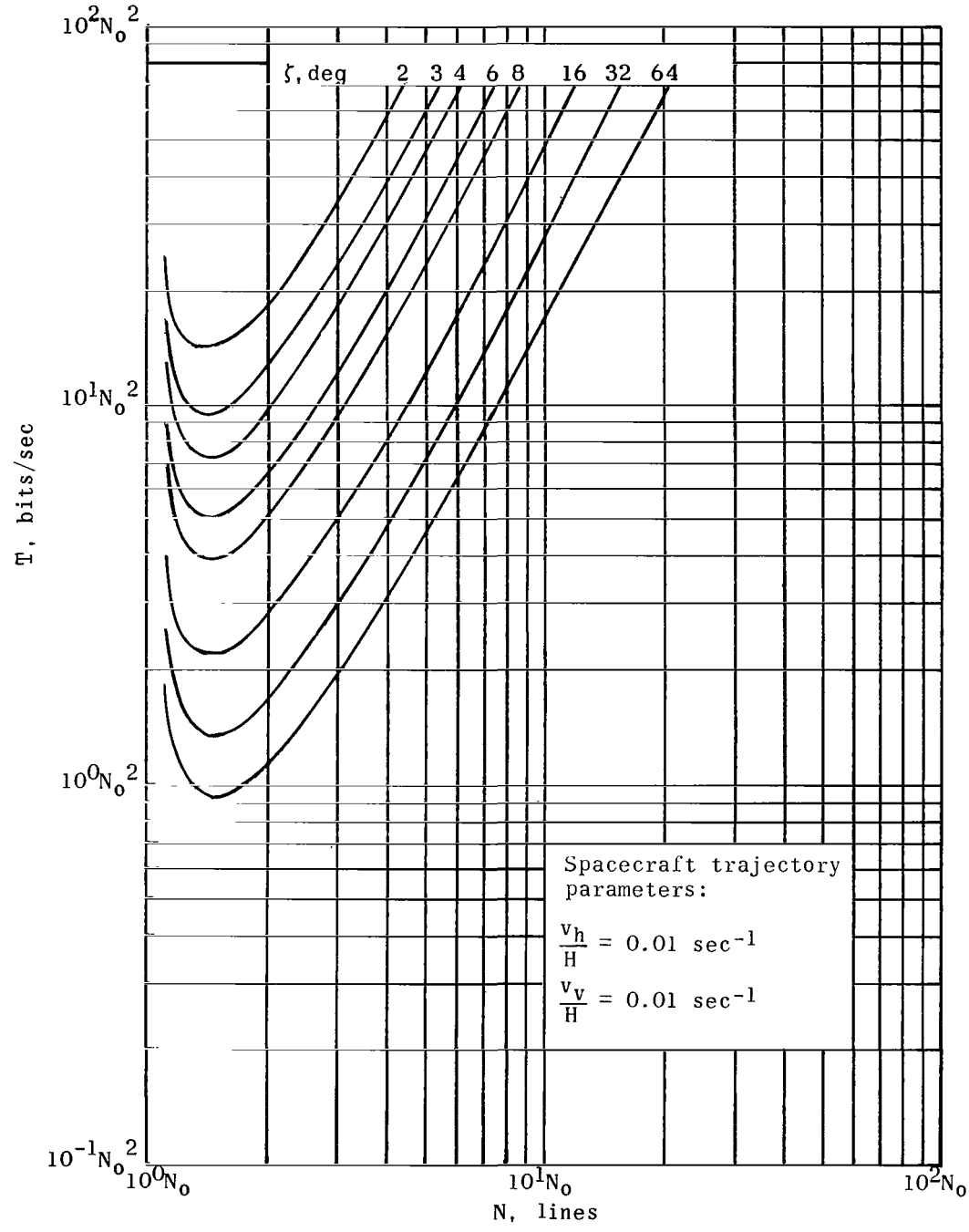

Figure 2.- Illustration of the variation of transmission rate required to secure N_o balanced lines overlap between successive pictures for changing optical field of view and number of balanced scan line values. Vidicon erase-and-prepare time is equal to readout time; viewing geometry is vertical.

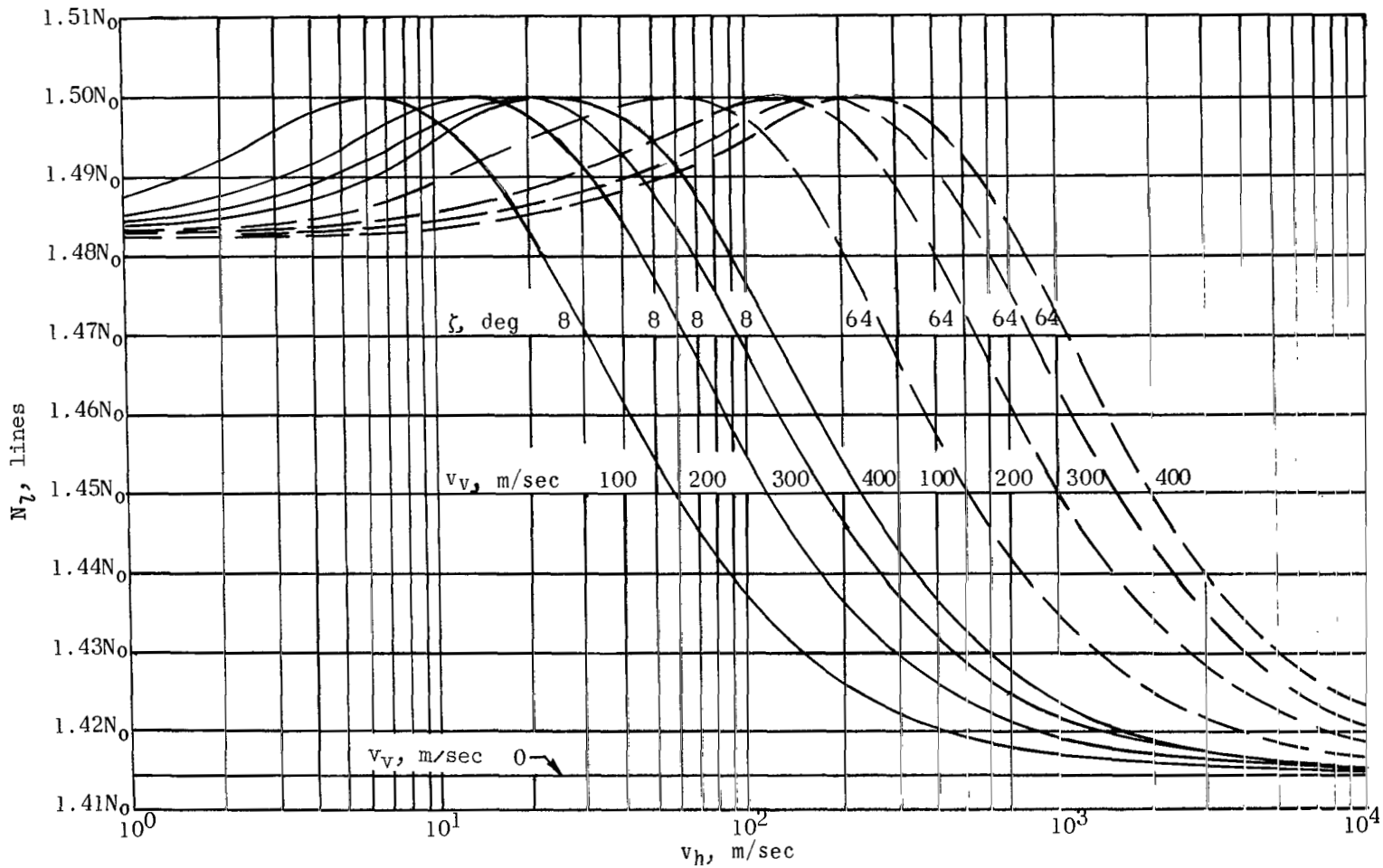

Figure 3.- Variation of N_ℓ with changes in spacecraft trajectory values and optical field of view.

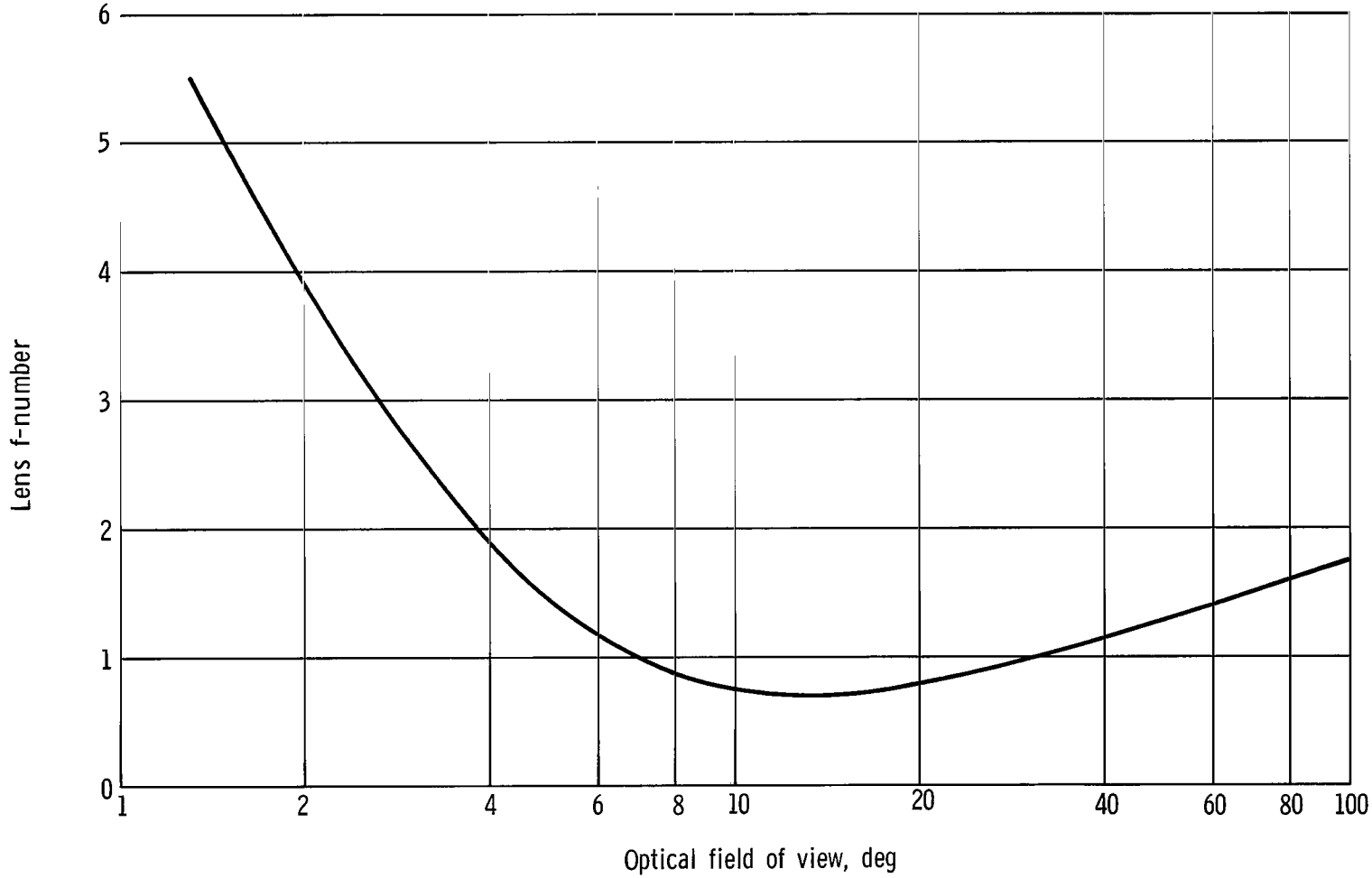

Figure 4.- Variation of lower limit of f-number for commercially available vidicon lenses with optical field-of-view (11.2-mm square vidicon format).

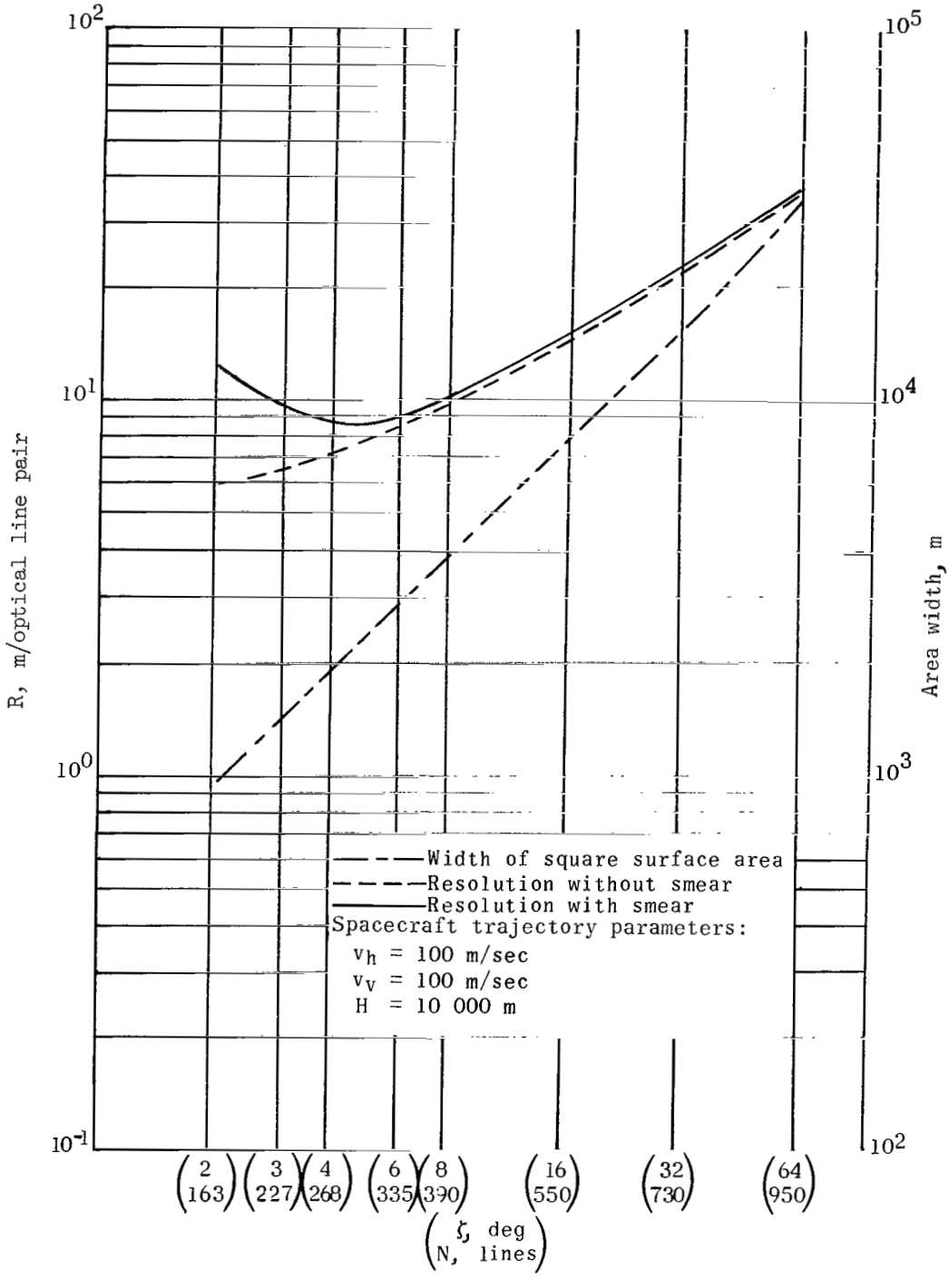

Figure 5.- Illustration of the variation of surface resolution and coverage for changing optical field of view and number of balanced scan lines. Successive pictures overlap by 100 balanced scan lines at a transmission rate of 150 000 bits/sec; vidicon erasure and prepare time is equal to readout time; viewing geometry is vertical.

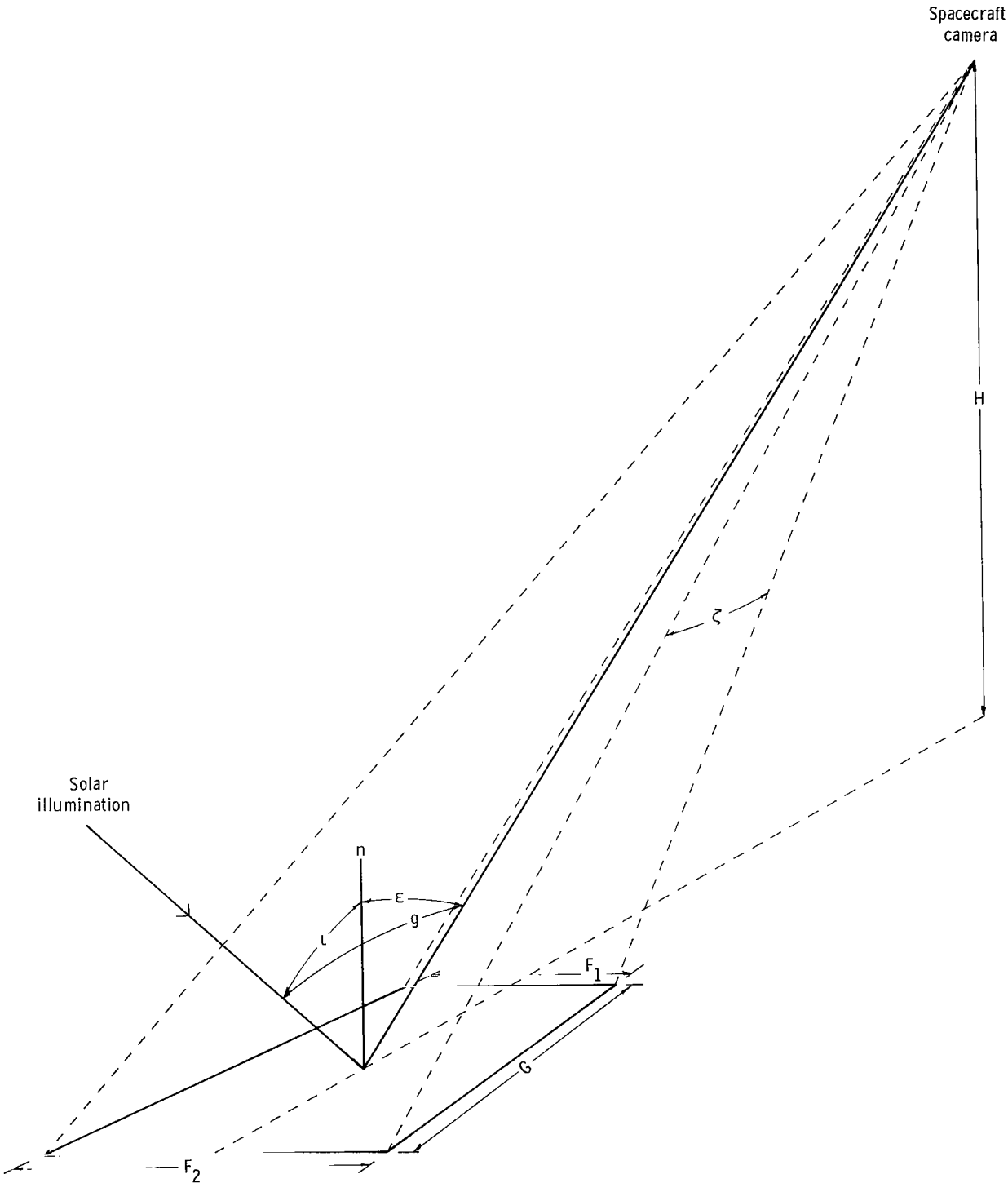

Figure 6.- Illustration of viewing geometry.

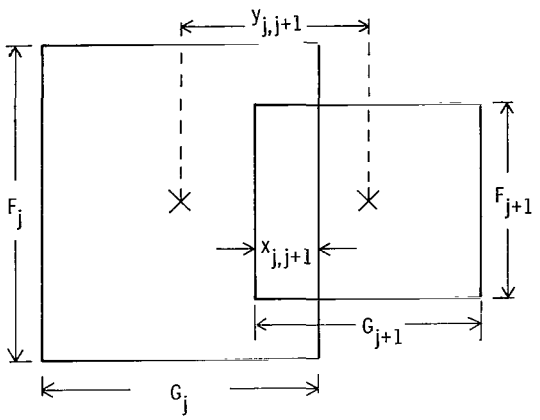

Figure 7.- Illustration of overlap requirement.

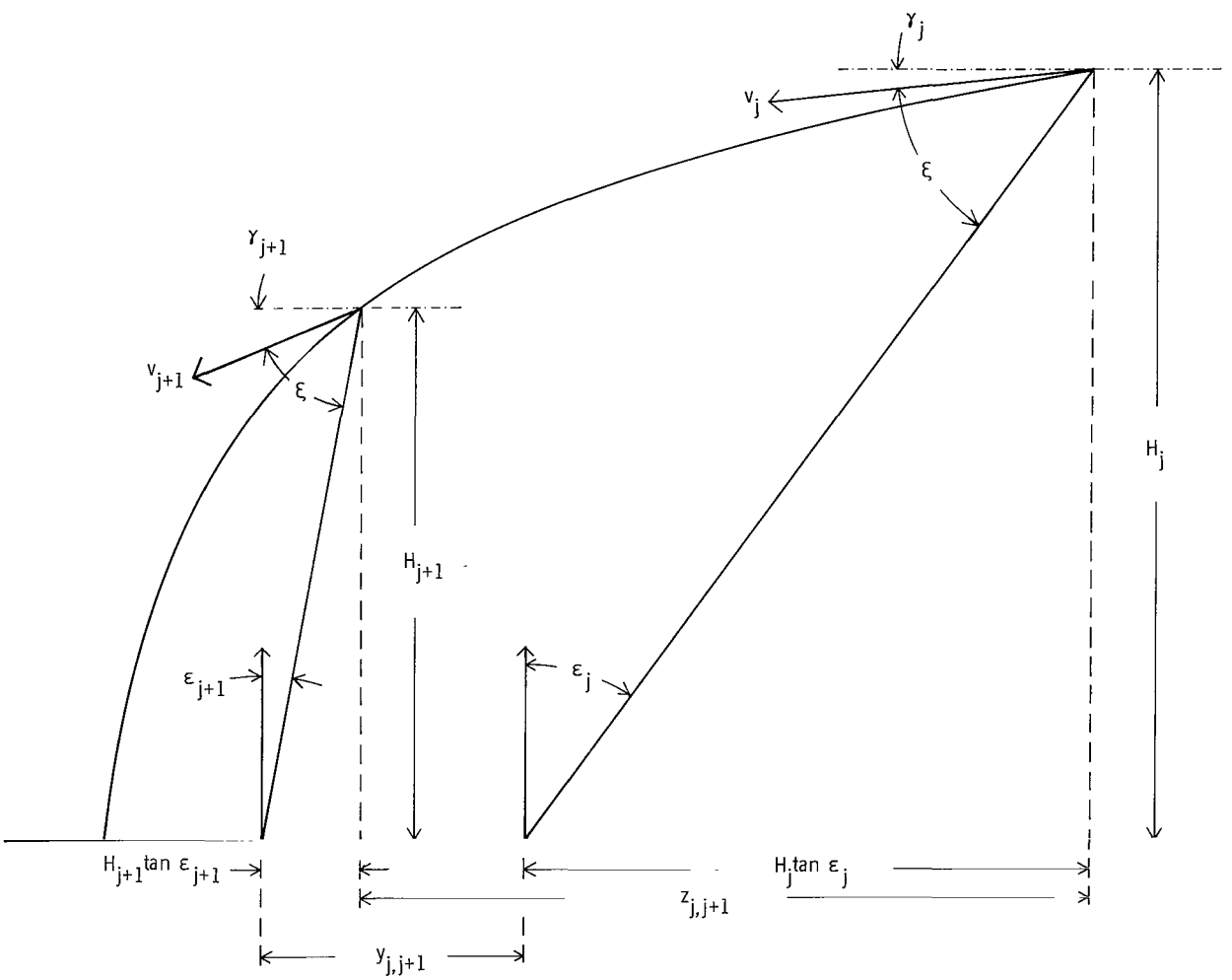

Figure 8.- Camera viewing geometry for two successive pictures.

NATIONAL AERONAUTICS AND SPACE ADMINISTRATION
WASHINGTON, D.C. 20546
OFFICIAL BUSINESS

FIRST CLASS MAIL

POSTAGE AND FEES PAID
NATIONAL AERONAUTICS AND
SPACE ADMINISTRATION

POSTMASTER: If Undeliverable (Section 158 Postal Manual) Do Not Return

"The aeronautical and space activities of the United States shall be conducted so as to contribute . . . to the expansion of human knowledge of phenomena in the atmosphere and space. The Administration shall provide for the widest practicable and appropriate dissemination of information concerning its activities and the results thereof."

— NATIONAL AERONAUTICS AND SPACE ACT OF 1958

NASA SCIENTIFIC AND TECHNICAL PUBLICATIONS

TECHNICAL REPORTS: Scientific and technical information considered important, complete, and a lasting contribution to existing knowledge.

TECHNICAL NOTES: Information less broad in scope but nevertheless of importance as a contribution to existing knowledge.

TECHNICAL MEMORANDUMS: Information receiving limited distribution because of preliminary data, security classification, or other reasons.

CONTRACTOR REPORTS: Scientific and technical information generated under a NASA contract or grant and considered an important contribution to existing knowledge.

TECHNICAL TRANSLATIONS: Information published in a foreign language considered to merit NASA distribution in English.

SPECIAL PUBLICATIONS: Information derived from or of value to NASA activities. Publications include conference proceedings, monographs, data compilations, handbooks, sourcebooks, and special bibliographies.

TECHNOLOGY UTILIZATION PUBLICATIONS: Information on technology used by NASA that may be of particular interest in commercial and other non-aerospace applications. Publications include Tech Briefs, Technology Utilization Reports and Notes, and Technology Surveys.

Details on the availability of these publications may be obtained from:

SCIENTIFIC AND TECHNICAL INFORMATION DIVISION

NATIONAL AERONAUTICS AND SPACE ADMINISTRATION

Washington, D.C. 20546